

# Driving collective RPA modes by a time-dependent Dyson map

---

Andreas Fring<sup>a</sup> Marta Reboiro<sup>b</sup>

<sup>a</sup>*Department of Mathematics, City St George's, University of London, Northampton Square, London EC1V 0HB, UK*

<sup>b</sup>*Institute of Physics of La Plata (IFLP), Boulevard 113 & 63, La Plata C.P. 1900, Argentina*

*E-mail:* [a.fring@city.ac.uk](mailto:a.fring@city.ac.uk), [reboiro@fisica.unlp.edu.ar](mailto:reboiro@fisica.unlp.edu.ar)

**ABSTRACT:** We study a time-dependent non-Hermitian generalisation of the Schütte-Da Providência model describing a bosonic mode coupled to collective particle-hole excitations. Using a time-dependent Dyson map, we construct a Hermitian counterpart and reduce the collective fermionic sector by means of the random phase approximation (RPA). The resulting dynamics is mapped to two time-dependent harmonic-oscillator branches with instantaneous RPA frequencies  $W_{\pm}(t)$ . We determine the corresponding stability regions and compute transition probabilities between instantaneous oscillator states. In first-order instantaneous-basis perturbation theory the leading transition  $n \rightarrow n + 2$  is proportional to  $\dot{W}_j/W_j$ , showing that it is purely nonadiabatic and absent in the time-independent case. We compare this result with exact Lewis-Riesenfeld transition amplitudes within the RPA approximation. Numerical examples show that different components of the Dyson map provide distinct driving mechanisms: the scaling parameter modulates the effective coupling, while the squeezing parameter acts through a moving-boundary contribution. In both cases the induced collective transitions exhibit parametric-resonance peaks and sideband structures.

**KEYWORDS:** Non-Hermitian spin-boson models; time-dependent Dyson maps; random phase approximation; collective RPA modes; squeezing transformations; moving boundaries; induced transitions

## 1 Introduction

In a recent work [1] we applied the general framework devised for the effective description of non-Hermitian Hamiltonian systems [2–5] to a time-dependent non-Hermitian Schütte-Da Providência spin-boson model [6] with moving-boundary interpretation. For explicitly time-dependent systems this structure becomes more subtle, since the time-dependence of the Dyson map contributes an additional gauge-like term to the Hermitian Hamiltonian [7, 8]. Time-independent pseudo-Hermitian versions of this model have been considered previously in [9]. For the setting considered in [1] the time-dependent Dyson map contained a bosonic squeezing transformation, whose time derivative produced a dilatation term. This term has the same structure as the inertial contribution that appears when a Hermitian system on a moving interval is transformed to a fixed reference interval. The main consequence was dynamical rather than spectral. In the fixed-boundary Hermitian model the operator  $Q = N - S_0$  is conserved, so that the spin-boson Hilbert space decomposes into independent sectors and transitions changing the boson number by two are forbidden. The moving-boundary term breaks this conservation law and opens  $n \leftrightarrow n \pm 2$  channels. For closed boundary protocols with constant background parameters the first-order integrated amplitude vanishes, whereas a time-dependent non-Hermitian deformation can change the dressed basis during the motion and thereby suppress or enhance the accumulated transition amplitude by coherent interference.

The present paper is a continuation of that analysis, but with a different emphasis. We do not study transitions between the finite-dimensional spin-boson sectors of the spin-1/2 model. Instead, we consider the collective many-fermion version of the Schütte-Da Providência model and reduce it by means of the random phase approximation (RPA) [10–16], see e.g. [17] for a recent review. The relevant degrees of freedom are then not individual spin-boson doublets, but collective particle-hole excitations of two degenerate fermionic shells coupled to a bosonic mode. After the Dyson transformation and the RPA reduction, the problem is mapped to time-dependent harmonic-oscillator branches. The central question therefore becomes how a time-dependent Dyson map can drive transitions between collective RPA oscillator states.

Originally the standard Schütte-Da Providência model was introduced as a solvable model of boson condensation. It describes a bosonic mode coupled to collective particle-hole excitations between two degenerate fermionic shells. The fermionic degrees of freedom can be represented by collective  $\mathfrak{su}(2)$  quasi-spin generators, with  $S_+$  creating a particle-hole excitation and  $S_-$  annihilating one. This makes the model a useful many-body analogue of spin-boson and light-matter Hamiltonians, while retaining enough algebraic structure to allow explicit calculations. In the collective regime, where the occupation of particle-hole excitations is small compared with the shell degeneracy, the Holstein-Primakoff representation [18] provides a natural route to a bosonic description of the fermionic sector.

The RPA is precisely designed for such small-amplitude collective dynamics. In its simplest form, it linearises the collective particle-hole motion around a reference configuration and replaces the relevant collective excitations by bosonic normal modes. It is widely used in many-body physics to describe collective vibrations, response functions and

stable small oscillations of interacting systems [17, 19–22]. In the present setting the RPA approximation converts the quasi-spin sector into an effective bosonic degree of freedom. The Dyson-transformed Schütte-Da Providência Hamiltonian then reduces to a quadratic bosonic Hamiltonian, whose normal modes are determined by an instantaneous RPA eigenvalue problem.

Introducing time-dependence and non-Hermiticity is motivated by two related points. First, time-dependent non-Hermitian Hamiltonians naturally arise as effective generators for driven systems, systems with controlled gain and loss, and systems described in time-dependent non-orthogonal representations. Secondly, in the quasi-Hermitian setting the time-dependence of the Dyson map is not merely a change of representation. It produces additional terms in the Hermitian frame and can therefore act as a genuine driving mechanism. In the present model the scaling part of the Dyson map modulates the effective coupling, whereas the squeezing part produces a moving-boundary contribution. Both mechanisms feed into the instantaneous RPA frequencies and can generate nonadiabatic transitions between oscillator states.

This provides the main difference from our previous work. There the moving-boundary term opened transitions between spin-boson sectors whose boson numbers differed by two. Here, after the collective RPA reduction, the induced transitions occur between instantaneous oscillator states of the RPA branches. The relevant transition amplitude is controlled by the time-dependence of the RPA frequency  $W_j(t)$ . In particular, the leading instantaneous-basis transition  $n \rightarrow n + 2$  is proportional to  $\dot{W}_j/W_j$  and therefore vanishes in the time-independent case. Thus the transition is not caused by the static Schütte-Da Providência interaction itself, but by the nonadiabatic driving induced through the time-dependent Dyson map.

The paper is organised as follows. In section 2 we introduce the time-dependent non-Hermitian Schütte-Da Providência Hamiltonian, construct its Hermitian Dyson-related counterpart and perform the RPA reduction using the Holstein-Primakoff representation. In section 3 we derive the instantaneous RPA frequency equation and identify the stable regions in which the collective branches have real positive frequencies. In section 4 we compute transition probabilities between instantaneous RPA oscillator states, first in instantaneous-basis perturbation theory and then exactly within the RPA approximation using Lewis-Riesenfeld invariants. In section 5 we illustrate the two driving mechanisms numerically: modulation of the Dyson-map scaling parameter and modulation of the squeezing, or moving-boundary, parameter. We summarise our conclusions in section 6.

## 2 Non-Hermitian Schütte-Da Providência model in RPA reduction

The Schütte-Da Providência model [6] describes a bosonic mode coupled to collective particle-hole excitations between two degenerate fermionic shells. In this work we consider a time-dependent non-Hermitian generalisation of the model, defined by the Hamiltonian

$$H(t) = \omega_f(t)S_0 + \omega_b(t)N_b + \alpha(t)S_+b^\dagger + \beta(t)S_-b, \quad \omega_f(t), \omega_b(t), \alpha(t), \beta(t) \in \mathbb{C}. \quad (2.1)$$

Throughout we use units in which  $\hbar = 1$ . Here  $b^\dagger$  and  $b$  are bosonic creation and annihilation operators satisfying  $[b, b^\dagger] = 1$ , and  $N_b = b^\dagger b$  is the boson number operator. The fermionic part of the model consists of two shells, labelled by 1 and 2, each with degeneracy  $2\Omega$ . We assume that the physical system contains  $2\Omega$  fermions. The corresponding collective particle-hole degrees of freedom are described by the collective quasi-spin operators

$$S_0 = \frac{1}{2} \sum_{k=1}^{2\Omega} (a_{2k}^\dagger a_{2k} - a_{1k}^\dagger a_{1k}) = \frac{1}{2} (N_f - 2\Omega), \quad S_+ = \sum_{k=1}^{2\Omega} a_{2k}^\dagger a_{1k}, \quad S_- = S_+^\dagger. \quad (2.2)$$

The operators  $a_{ik}^\dagger$  and  $a_{ik}$ , with  $i = 1, 2$  and  $k = 1, \dots, 2\Omega$ , are fermionic creation and annihilation operators. The quasi-spin generators satisfy the  $\mathfrak{su}(2)$ -algebra  $[S_0, S_\pm] = \pm S_\pm$ ,  $[S_+, S_-] = 2S_0$ . In the expression for  $S_0$ ,  $N_f$  denotes the number of upper-level particles plus lower-level holes, namely

$$N_f = \sum_{k=1}^{2\Omega} (a_{2k}^\dagger a_{2k} + a_{1k} a_{1k}^\dagger). \quad (2.3)$$

The Hermitian Schütte-Da Providência model is recovered when  $\omega_f(t)$  and  $\omega_b(t)$  are real and the two interaction strengths satisfy  $\beta(t) = \alpha^*(t)$ . In the non-Hermitian case considered here, the parameters are allowed to be complex and, in particular,  $\alpha(t)$  and  $\beta(t)$  are independent. The latter choice describes an asymmetric coupling between the creation and annihilation of a boson and a collective particle-hole excitation.

In [1] we constructed a Hermitian counterpart

$$h(t) = (\omega_f + i\dot{\delta}) S_0 + (\omega_b + i\dot{\gamma}) \left[ \cosh(2\kappa) N_b - \frac{1}{2} \sinh(2\kappa) (b^{\dagger 2} + b^2) + \sinh^2(\kappa) \right] \\ + \alpha e^{\gamma+\delta} S_+ (b^\dagger \cosh \kappa - b \sinh \kappa) + \beta e^{-(\gamma+\delta)} S_- (b \cosh \kappa - b^\dagger \sinh \kappa) + i \frac{\dot{\kappa}}{2} (b^{\dagger 2} - b^2), \quad (2.4)$$

by solving the time-dependent Dyson equation

$$h(t) = \eta(t) H(t) \eta^{-1}(t) + i \dot{\eta}(t) \eta^{-1}(t), \quad (2.5)$$

for the time-dependent Dyson map

$$\eta(t) := e^{\kappa(t)(b^{\dagger 2} - b^2)/2} e^{\gamma(t) N_b} e^{\delta(t) S_0}, \quad \kappa(t), \gamma(t), \delta(t) \in \mathbb{C}, \quad (2.6)$$

Here and below the time dependence of  $\gamma, \delta, \kappa$  is understood.

The Hamiltonian  $h(t)$  is Hermitian provided the conditions

$$A_f(t) := \omega_f + i\dot{\delta} \in \mathbb{R}, \quad A_b(t) := \omega_b + i\dot{\gamma} \in \mathbb{R}, \quad \kappa \in \mathbb{R}, \quad \beta = \alpha^* e^{2\Re(\gamma+\delta)}. \quad (2.7)$$

In addition, the metric and its inverse remain bounded, for instance, when  $\gamma(t) \in i\mathbb{R}$ . These conditions ensure that the transformed Hamiltonian defines a unitary evolution in the Dyson-related Hermitian frame.

For our purposes here it is useful to introduce the squeezed bosonic operators by means of a Bogoliubov transformation

$$B^\dagger = b^\dagger \cosh \kappa(t) - b \sinh \kappa(t), \quad B = b \cosh \kappa(t) - b^\dagger \sinh \kappa(t), \quad (2.8)$$

satisfying the usual bosonic commutation relation  $[B, B^\dagger] = 1$ . In terms of these operators the Hamiltonian takes the compact form

$$h(t) = A_f(t)S_0 + A_b(t)B^\dagger B + g(t)S_+ B^\dagger + g^*(t)S_- B + \frac{i\dot{\kappa}(t)}{2} (B^{\dagger 2} - B^2), \quad (2.9)$$

where  $g(t) := \alpha(t)e^{\gamma(t)+\delta(t)}$ . This form makes the role of the Dyson map transparent. The function  $\delta(t)$  rescales the effective coupling  $g(t)$ , while  $\kappa(t)$  enters both through the squeezed boson  $B$  and through the explicitly time-dependent boundary term proportional to  $\dot{\kappa}(t)$ .

We now pass to a random phase approximation [10–12], see e.g. [17] for a recent review. The basic assumption is that the collective sector dominates the dynamics. To leading order, the fermionic operators may be bosonised by means of the Holstein-Primakoff representation [18],

$$S_+ = \sqrt{2\Omega} a^\dagger \left(1 - \frac{a^\dagger a}{2\Omega}\right)^{1/2} \simeq \sqrt{2\Omega} a^\dagger, \quad (2.10)$$

$$S_- = \sqrt{2\Omega} \left(1 - \frac{a^\dagger a}{2\Omega}\right)^{1/2} a \simeq \sqrt{2\Omega} a, \quad (2.11)$$

$$S_0 = a^\dagger a - \Omega. \quad (2.12)$$

This RPA approximation is valid for low collective occupations

$$\langle a^\dagger a \rangle \ll 2\Omega. \quad (2.13)$$

In the commutators generated by the interaction terms we use, consistently with  $a^\dagger a \ll 2\Omega$ , the leading approximation  $S_0 \simeq -\Omega$ . Up to an irrelevant constant, the Hamiltonian (2.9) then becomes a quadratic bosonic Hamiltonian. The corresponding collective RPA excitation is taken in the form

$$\Gamma^\dagger := X_1 S_+ - Y_1 S_- + X_2 B^\dagger - Y_2 B, \quad (2.14)$$

with normalisation condition

$$[\Gamma, \Gamma^\dagger] = 1, \quad (2.15)$$

which holds when the constants  $X_1, X_2, Y_1, Y_2$  are constrained as

$$2\Omega (|X_1|^2 - |Y_1|^2) + |X_2|^2 - |Y_2|^2 = 1. \quad (2.16)$$

The RPA frequencies  $W(t)$  are determined by the equation of motion

$$[h(t), \Gamma^\dagger] = W(t)\Gamma^\dagger. \quad (2.17)$$

This is the instantaneous RPA eigenvalue problem for the collective mode. It leads to the secular equation for the two RPA frequencies  $W_\pm(t)$ , which will be analysed in the next section. Only those branches for which the frequencies are real and positive give stable oscillator modes.

For each stable RPA branch the collective Hamiltonian may be represented as a time-dependent harmonic oscillator. Introducing canonical variables  $\hat{x}_j, \hat{p}_j$ , one may write

$$\Gamma_j^\dagger = \sqrt{\frac{mW_j(t)}{2}} \left( \hat{x}_j - \frac{i}{mW_j(t)} \hat{p}_j \right), \quad \Gamma_j = \sqrt{\frac{mW_j(t)}{2}} \left( \hat{x}_j + \frac{i}{mW_j(t)} \hat{p}_j \right), \quad (2.18)$$

so that the RPA Hamiltonian for branch  $j = \pm$  takes the form of the harmonic oscillator with time-dependent frequency

$$H_{\text{RPA},j}(t) = \frac{\hat{p}_j^2}{2m} + \frac{m}{2} W_j^2(t) \hat{x}_j^2. \quad (2.19)$$

Thus the time-dependent non-Hermitian spin-boson problem, after the Dyson transformation and the RPA reduction, is mapped to two time-dependent oscillator branches. This oscillator form can be solved exactly using Lewis-Riesenfeld invariants [23–25]. It is the starting point for both the perturbative and the exact transition-probability calculations below.

### 3 Stable RPA regions

The equation of motion (2.17) can be written explicitly as a finite-dimensional RPA eigenvalue problem. Suppressing the time dependence and using the RPA replacements (2.10)–(2.12), the relevant commutators are

$$[h, S_+]_{\text{RPA}} = A_f S_+ + 2\Omega g^* B, \quad [h, S_-]_{\text{RPA}} = -A_f S_- - 2\Omega g B^\dagger, \quad (3.1)$$

$$[h, B^\dagger] = A_b B^\dagger + g^* S_- - i\kappa B, \quad [h, B] = -A_b B - g S_+ - i\kappa B^\dagger. \quad (3.2)$$

Substitution of  $\Gamma^\dagger$  from (2.14) then gives

$$\mathcal{M}_{\text{RPA}} \begin{pmatrix} X_1 \\ Y_1 \\ X_2 \\ Y_2 \end{pmatrix} = W \begin{pmatrix} X_1 \\ Y_1 \\ X_2 \\ Y_2 \end{pmatrix}, \quad (3.3)$$

where

$$\mathcal{M}_{\text{RPA}} = \begin{pmatrix} A_f & 0 & 0 & g \\ 0 & -A_f & -g^* & 0 \\ 0 & 2\Omega g & A_b & i\kappa \\ -2\Omega g^* & 0 & i\kappa & -A_b \end{pmatrix}. \quad (3.4)$$

The secular condition  $\det(\mathcal{M}_{\text{RPA}} - W\mathbb{I}) = 0$  then yields the determining equation for the RPA frequencies

$$(W^2 - A_f^2) (\kappa^2 + W^2 - A_b^2) + 4\Omega|g|^2 (W^2 - A_b A_f) + 4\Omega^2|g|^4 = 0. \quad (3.5)$$

Solving this fourth order equation and keeping only the positive frequencies gives

$$W_\pm(t) = \sqrt{\frac{A_f(t)^2 + A_b(t)^2 - \kappa(t)^2 - 4\Omega|g(t)|^2 \pm \sqrt{\Delta(t)}}{2}} \quad (3.6)$$

with discriminant

$$\Delta(t) = [A_f(t)^2 - A_b(t)^2 + \dot{\kappa}(t)^2]^2 - 8\Omega|g(t)|^2 [(A_f(t) - A_b(t))^2 - \dot{\kappa}(t)^2]. \quad (3.7)$$

Only those branches for which  $\Delta(t) \geq 0$ ,  $W_{\pm}(t)^2 > 0$  are stable real oscillator frequencies. A rough estimate of the allowed region is obtained from the special case  $\dot{\kappa}(t) = 0$ , for which the discriminant becomes

$$\Delta_0 = (A_f - A_b)^2 [(A_f + A_b)^2 - 8\Omega|g|^2]. \quad (3.8)$$

Thus, the static estimate is

$$8\Omega|g|^2 \leq (A_f + A_b)^2. \quad (3.9)$$

At equality, one of the RPA modes may become soft. Beyond this region, the RPA frequencies become complex, signalling an instability or breakdown of the RPA approximation. For genuinely time-dependent boundaries this condition should only be used as a static estimate. In the numerical analysis below we impose the full instantaneous conditions  $\Delta(t) \geq 0$  and  $W_{\pm}^2(t) > 0$  over the full time interval.

## 4 RPA transition probabilities: perturbative and exact

### 4.1 Instantaneous-basis perturbation theory

At each fixed time  $t$ , the instantaneous eigenvalue problem for the RPA Hamiltonian  $H_{\text{RPA},j}(t)$  in (2.19) is

$$H_{\text{RPA},j}(t)|n, j; t\rangle = E_{n,j}(t)|n, j; t\rangle, \quad (4.1)$$

with instantaneous eigenstates  $|n, j; t\rangle$  and instantaneous eigenenergies

$$E_{n,j}(t) = W_j(t) \left( n + \frac{1}{2} \right), \quad n = 0, 1, 2, \dots \quad (4.2)$$

We expand an arbitrary state in the instantaneous basis as

$$|\Psi_j(t)\rangle = \sum_n c_n^{(j)}(t) \exp \left[ -i \int_0^t ds E_{n,j}(s) \right] |n, j; t\rangle. \quad (4.3)$$

Substituting this into the Schrödinger equation

$$i \frac{d}{dt} |\Psi_j(t)\rangle = H_{\text{RPA},j}(t) |\Psi_j(t)\rangle \quad (4.4)$$

gives

$$\dot{c}_m^{(j)}(t) = - \sum_n c_n^{(j)}(t) \langle m, j; t | \partial_t | n, j; t \rangle \exp \left[ i \int_0^t ds (E_{m,j}(s) - E_{n,j}(s)) \right]. \quad (4.5)$$

To first order, for an initial state  $|n, j; 0\rangle$ , we set

$$c_n^{(j)}(t) \simeq 1, \quad c_{m \neq n}^{(j)}(t) \simeq 0. \quad (4.6)$$

Hence the transition amplitude from  $n$  to  $m$  is

$$A_{m \leftarrow n}^{(j)}(T) \simeq - \int_0^T dt \langle m, j; t | \partial_t n, j; t \rangle \exp \left[ i \int_0^t ds (E_{m,j}(s) - E_{n,j}(s)) \right]. \quad (4.7)$$

Next we compute the nonadiabatic matrix element  $\langle m, j; t | \partial_t n, j; t \rangle$ . We start by differentiating the instantaneous eigenvalue equation (4.1). Projecting with  $\langle m, j; t |$  for  $m \neq n$ , gives

$$\langle m, j; t | \partial_t n, j; t \rangle = \frac{\langle m, j; t | \partial_t H_{\text{RPA},j}(t) | n, j; t \rangle}{E_{n,j}(t) - E_{m,j}(t)}. \quad (4.8)$$

With the expression (2.19) for the RPA Hamiltonian we get

$$\partial_t H_{\text{RPA},j}(t) = m W_j(t) \dot{W}_j(t) \hat{x}_j^2. \quad (4.9)$$

Using the instantaneous oscillator representation

$$\hat{x}_j = \sqrt{\frac{1}{2mW_j(t)}} (a_j + a_j^\dagger), \quad (4.10)$$

we obtain

$$\langle n+2, j; t | \hat{x}_j^2 | n, j; t \rangle = \frac{1}{2mW_j(t)} \sqrt{(n+1)(n+2)}. \quad (4.11)$$

Therefore

$$\langle n+2, j; t | \partial_t H_{\text{RPA},j}(t) | n, j; t \rangle = \frac{\dot{W}_j(t)}{2} \sqrt{(n+1)(n+2)}. \quad (4.12)$$

Together with

$$E_{n+2,j}(t) - E_{n,j}(t) = 2W_j(t). \quad (4.13)$$

this gives, up to a phase convention, for the instantaneous eigenstates,

$$\langle n+2, j; t | \partial_t n, j; t \rangle = - \frac{\dot{W}_j(t)}{4W_j(t)} \sqrt{(n+1)(n+2)}. \quad (4.14)$$

With the opposite phase convention this matrix element appears with the opposite sign. The sign is immaterial for the transition probability. Equation (4.14) shows explicitly that the  $n \rightarrow n+2$  transition is purely nonadiabatic: it is generated by the time dependence of the instantaneous RPA basis and is proportional to  $\dot{W}_j(t)$ . Hence, in the time-independent case, where  $W_j$  is constant, no  $n \rightarrow n+2$  transition is induced.

Thus we have

$$A_{n+2 \leftarrow n}^{(j)}(T) \simeq - \frac{\sqrt{(n+1)(n+2)}}{4} \int_0^T dt \frac{\dot{W}_j(t)}{W_j(t)} \exp \left[ 2i \int_0^t ds W_j(s) \right]. \quad (4.15)$$

The corresponding transition probability is

$$P_{n+2 \leftarrow n}^{(j)}(T) \simeq \left| A_{n+2 \leftarrow n}^{(j)}(T) \right|^2. \quad (4.16)$$

This expression should be understood as a first-order perturbative transition probability. It was obtained by expanding the state in the instantaneous oscillator basis and

retaining only the leading nonadiabatic coupling between  $|n, j; t\rangle$  and  $|n+2, j; t\rangle$ . Consequently, the result is reliable only when the corresponding transition amplitude remains small, i.e.  $|A_{n+2\leftarrow n}^{(j)}(T)| \ll 1$ . Thus if the expression for  $P_{n+2\leftarrow n}^{(j)}(T)$  becomes comparable to or larger than unity, this signals the breakdown of the first-order approximation rather than a physical probability exceeding one or a missing normalisation factor. In addition, in the RPA setting we need to remain within the range of validity of the bosonised approximation, namely occupations satisfying  $n \ll 2\Omega$ .

## 4.2 Exact Lewis-Riesenfeld transition amplitudes

Using the RPA oscillator reduction described above, we can compare the perturbative analysis with the exact analytic solution within the RPA approximation. For a given branch  $j$ , the exact solution that solves the full time-dependent Schrödinger equation can be written in terms of the Lewis-Riesenfeld invariant

$$\Psi_n^{(j)}(x, t) = e^{-i(n+1/2)\theta_j(t)} \frac{1}{\sqrt{2^n n!}} \left( \frac{1}{\pi \rho_j^2(t)} \right)^{1/4} H_n \left( \frac{x}{\rho_j(t)} \right) e^{\frac{1}{2\rho_j^2(t)} [im\dot{\rho}_j(t)\rho_j(t) - 1]x^2}, \quad (4.17)$$

where

$$\theta_j(t) = \int_0^t \frac{dt'}{m\rho_j^2(t')}, \quad (4.18)$$

and  $\rho_j(t)$  is a real solution of the Ermakov-Pinney equation

$$\ddot{\rho}_j(t) + W_j^2(t)\rho_j(t) = \frac{1}{m^2\rho_j^3(t)}. \quad (4.19)$$

The eigenfunctions of the instantaneous Hamiltonian  $H_j(t)$  are the ordinary harmonic-oscillator eigenfunctions with frequency  $W_j(t)$ .

$$\phi_{n,j}(x; t) = \frac{1}{\sqrt{2^n n!}} \left( \frac{mW_j(t)}{\pi} \right)^{1/4} H_n \left( \sqrt{mW_j(t)} x \right) \exp \left[ -\frac{mW_j(t)x^2}{2} \right]. \quad (4.20)$$

Thus, choosing the initial values

$$\rho_j(0) = \frac{1}{\sqrt{mW_j(0)}}, \quad \dot{\rho}_j(0) = 0, \quad (4.21)$$

ensures that  $\Psi_n^{(j)}(x, 0) = \phi_{n,j}(x; 0)$ . Then, the exact transition amplitude from the initial instantaneous state  $\phi_{n,j}(x; 0)$  to the state  $\phi_{n+2,j}(x; T)$  is given as

$$A_{n+2\leftarrow n}^{(j)}(T) = \int_{-\infty}^{\infty} dx \phi_{n+2,j}^*(x; T) \Psi_n^{(j)}(x, T). \quad (4.22)$$

Next we compute this expression. Suppressing the branch label  $j$  and abbreviating at the final time  $T$

$$q := \sqrt{mW(T)}, \quad r := \frac{1}{\rho(T)}, \quad s := m \frac{\dot{\rho}(T)}{\rho(T)}, \quad C := q^2 + r^2 - is. \quad (4.23)$$

we obtain

$$A_{n+2\leftarrow n}(T) = e^{-i(n+1/2)\theta(T)} \frac{1}{\sqrt{2^{2n+2}(n+2)!n!}} \sqrt{\frac{qr}{\pi}} I_n, \quad (4.24)$$

where

$$I_n = \int_{-\infty}^{\infty} dx H_{n+2}(qx) H_n(rx) \exp\left[-\frac{Cx^2}{2}\right]. \quad (4.25)$$

We evaluate this integral using the generating function for the Hermite polynomials

$$e^{-u^2+2uy} = \sum_{m=0}^{\infty} \frac{u^m}{m!} H_m(y). \quad (4.26)$$

Accordingly, we can express the two Hermite polynomials in the integrand as

$$H_{n+2}(qx) = \partial_u^{n+2} e^{-u^2+2uqx} \Big|_{u=0}, \quad H_n(rx) = \partial_v^n e^{-v^2+2vrx} \Big|_{v=0}. \quad (4.27)$$

Therefore, the integral becomes

$$I_n = \partial_u^{n+2} \partial_v^n \int_{-\infty}^{\infty} dx \exp\left[-\frac{Cx^2}{2} - u^2 - v^2 + 2x(qu + rv)\right] \Big|_{u=v=0}. \quad (4.28)$$

The  $x$ -integral is elementary, so that we obtain

$$I_n = \sqrt{\frac{2\pi}{C}} \frac{\partial^{n+2}}{\partial u^{n+2}} \frac{\partial^n}{\partial v^n} \exp[au^2 + cuv + bv^2] \Big|_{u=v=0}, \quad (4.29)$$

with

$$a = \frac{2q^2}{C} - 1, \quad b = \frac{2r^2}{C} - 1, \quad c = \frac{4qr}{C}. \quad (4.30)$$

Expanding the exponential functions as

$$e^{au^2} = \sum_{p=0}^{\infty} \frac{a^p u^{2p}}{p!}, \quad e^{cuv} = \sum_{k=0}^{\infty} \frac{c^k u^k v^k}{k!}, \quad e^{bv^2} = \sum_{\ell=0}^{\infty} \frac{b^\ell v^{2\ell}}{\ell!}, \quad (4.31)$$

we note that the derivative  $\partial_u^{n+2} \partial_v^n$  selects the coefficient of  $u^{n+2} v^n$ , so that we require

$$2p + k = n + 2, \quad k + 2\ell = n, \quad \Rightarrow \quad p = \ell + 1, \quad \ell = 0, 1, \dots, \left\lfloor \frac{n}{2} \right\rfloor. \quad (4.32)$$

The coefficient of  $u^{n+2} v^n$  is therefore

$$\sum_{\ell=0}^{\lfloor n/2 \rfloor} \frac{a^{\ell+1} b^\ell c^{n-2\ell}}{(\ell+1)! \ell! (n-2\ell)!}, \quad (4.33)$$

so that

$$I_n = \sqrt{\frac{2\pi}{C}} (n+2)! n! \sum_{\ell=0}^{\lfloor n/2 \rfloor} \frac{a^{\ell+1} b^\ell c^{n-2\ell}}{(\ell+1)! \ell! (n-2\ell)!}. \quad (4.34)$$

Restoring the branch label  $j$ , the exact RPA transition amplitude becomes

$$A_{n+2\leftarrow n}^{(j),\text{exact}}(T) = e^{-i(n+1/2)\theta_j(T)} \sqrt{\frac{2q_j r_j}{C_j}} \frac{\sqrt{(n+2)! n!}}{2^{n+1}} \sum_{\ell=0}^{\lfloor n/2 \rfloor} \frac{a_j^{\ell+1} b_j^\ell c_j^{n-2\ell}}{(\ell+1)! \ell! (n-2\ell)!}. \quad (4.35)$$

For the special cases  $n = 0$  and  $n = 2$  the expressions simplify to

$$A_{2\leftarrow 0}^{(j),\text{exact}}(T) = e^{-i\theta_j(T)/2} \sqrt{\frac{q_j r_j}{C_j}} a_j, \quad (4.36)$$

$$A_{4\leftarrow 2}^{(j),\text{exact}}(T) = \frac{1}{2} \sqrt{\frac{3}{2}} e^{-5i\theta_j(T)/2} \sqrt{\frac{q_j r_j}{C_j}} a_j (a_j b_j + c_j^2). \quad (4.37)$$

The corresponding exact RPA transition probability is therefore

$$P_{n+2\leftarrow n}^{(j),\text{exact}}(T) = \left| A_{n+2\leftarrow n}^{(j),\text{exact}}(T) \right|^2. \quad (4.38)$$

### 4.3 Weak-driving limit and comparison

In the weak-driving regime the Lewis-Riesenfeld result reduces to the first-order instantaneous-basis expression. The reason is that a slowly or weakly varying frequency  $W_j(t)$  produces only a small mismatch between the exact evolved state and the final instantaneous oscillator basis. Equivalently, the squeezing parameters encoded in  $a_j, b_j, c_j$  remain small, and the dominant contribution to the transition amplitude is the direct  $n \rightarrow n+2$  nonadiabatic coupling proportional to  $\dot{W}_j/W_j$ . Thus the perturbative expression captures the leading resonance structure, while the exact expression contains the higher-order squeezing corrections and the depletion of the initial state. This distinction becomes important near strong resonances, where the perturbative probability can overestimate the exact transition probability even though it continues to predict the correct peak positions.

## 5 Numerical analysis

We now use the expressions from the previous section to analyse two complementary driving mechanisms. The first mechanism is driven by the scaling part of the Dyson map: the parameter  $\delta(t)$  is modulated in time and its modulation frequency is scanned, while the boundary protocol  $\kappa(t)$  is kept fixed. Since  $\delta(t)$  enters the effective coupling  $|g(t)|$ , this produces a time-dependent RPA frequency and hence nonadiabatic transitions between instantaneous oscillator states. The second mechanism is driven by the squeezing part of the Dyson map:  $\delta$  is kept fixed, but the boundary parameter  $\kappa(t)$  is varied periodically. In this case the transition is generated directly by the moving-boundary contribution to  $W_+(t)$ . In both cases the peaks in the transition probability can be understood as parametric resonances, while the smaller neighbouring peaks arise from sideband mixing with the additional modulation of  $A_b(t)$ .

### 5.1 Dyson-map driven transition probability

Figure 1 displays the RPA transition probability  $P_{2\leftarrow 0}^{(+)}(T)$  as a function of the Dyson-map modulation frequency  $\omega_\delta$  in the perturbative approximation (4.16) and exact analytical form (4.38). The parameter  $\delta(t) = \delta_0 + d_0 \sin(\omega_\delta t)$  enters the effective coupling as

$$|g(t)| = \frac{\lambda e^{\delta(t)}}{\sqrt{2\Omega}}, \quad (5.1)$$

and therefore modulates the instantaneous RPA frequency  $W_+(t)$ . This time dependence generates the nonadiabatic coupling between instantaneous oscillator states responsible for the transition  $0 \rightarrow 2$ .

The dominant peak occurs when the modulation frequency satisfies the parametric resonance condition

$$\omega_\delta \simeq 2\overline{W}_+, \quad \overline{W}_+ = \frac{1}{T} \int_0^T W_+(t) dt. \quad (5.2)$$

This reflects the fact that the transition  $0 \rightarrow 2$  has energy gap  $2W_+$ . The smaller peaks arise as sideband resonances, generated by the additional modulation of the RPA frequency through  $A_b(t) = 1 + 0.08 \cos(\omega_b t)$ . They are expected near

$$\omega_\delta \simeq 2\overline{W}_+ \pm \omega_b. \quad (5.3)$$

For the parameters of figure 1, this gives sideband peaks near  $\omega_\delta \simeq 1.54$  and  $\omega_\delta \simeq 2.04$ , surrounding the dominant resonance near  $\omega_\delta \simeq 1.79$ . The figure therefore shows that the transition can be driven directly by the time-dependent Dyson map. By tuning  $\omega_\delta$ , the integrated transition amplitude can be enhanced or suppressed through constructive or destructive phase interference.

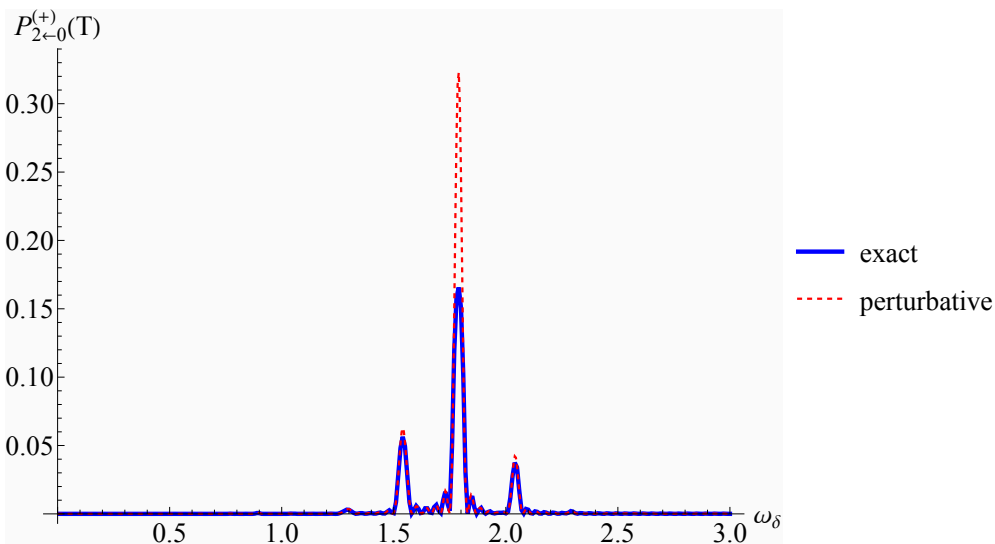


**Figure 1.** Dyson-map driven transition probability  $P_{2\leftarrow 0}^{(+)}(T)$  in the perturbative approximation (4.16) and exact analytical form (4.38) as a function of the modulation frequency  $\omega_\delta$ . The parameters are  $A_f(t) = 0$ ,  $A_b(t) = 1 + 0.08 \cos(\omega_b t)$ ,  $\kappa(t) = \kappa_0 \sin(\omega_\kappa t)$ ,  $\delta(t) = \delta_0 + d_0 \sin(\omega_\delta t)$ ,  $|g(t)| = \lambda e^{\delta(t)} / \sqrt{2\Omega}$ ,  $\omega_b = 0.25$ ,  $\kappa_0 = 0.05$ ,  $\omega_\kappa = 0.8$ ,  $\delta_0 = 0.2$ ,  $d_0 = 0.05$ ,  $\lambda = 0.25$ ,  $T = 2\pi 20 / \omega_\kappa$ , and  $\Omega = 25$ . The dominant peak occurs near  $\omega_\delta \simeq 1.79$ , while the smaller sideband peaks occur near  $\omega_\delta \simeq 1.54$  and  $\omega_\delta \simeq 2.04$ .

We find that the exact Lewis-Riesenfeld result agrees well with the first-order nonadiabatic expression in the weak-driving regime. For stronger driving, especially near the dominant resonance, the perturbative result overestimates the transition probability as seen in figure 1 because the first-order approximation neglects depletion of the initial state,

i.e. it keeps  $c_n^{(j)}(t) \simeq 1$  in (4.6), and higher-order squeezing-induced redistribution among the even oscillator levels. This explains why the perturbative and exact curves have the same resonance positions but different peak heights.

## 5.2 Boundary driven transition probability

Figure 2 displays the RPA transition probability  $P_{4\leftarrow 2}^{(+)}(T)$  as a function of the boundary modulation frequency  $\omega_\kappa$  in the perturbative approximation (4.16) and exact analytical form (4.38). In this case the Dyson map scaling parameter is kept fixed,  $\delta(t) = \delta_0$ , so that the effective coupling

$$|g(t)| = \frac{\lambda e^{\delta_0}}{\sqrt{2\Omega}} \quad (5.4)$$

is time independent. The transition is instead driven by the squeezing part of the Dyson map through  $\kappa(t) = \kappa_0 \sin(\omega_\kappa t)$ . Since the instantaneous RPA frequency depends on  $\dot{\kappa}(t)^2$ , the boundary motion contributes through

$$\dot{\kappa}(t)^2 = \kappa_0^2 \omega_\kappa^2 \cos^2(\omega_\kappa t) = \frac{\kappa_0^2 \omega_\kappa^2}{2} [1 + \cos(2\omega_\kappa t)]. \quad (5.5)$$

Thus the moving boundary modulates  $W_+(t)$  predominantly at frequency  $2\omega_\kappa$ , generating the nonadiabatic coupling between instantaneous oscillator states responsible for the transition  $2 \rightarrow 4$ .

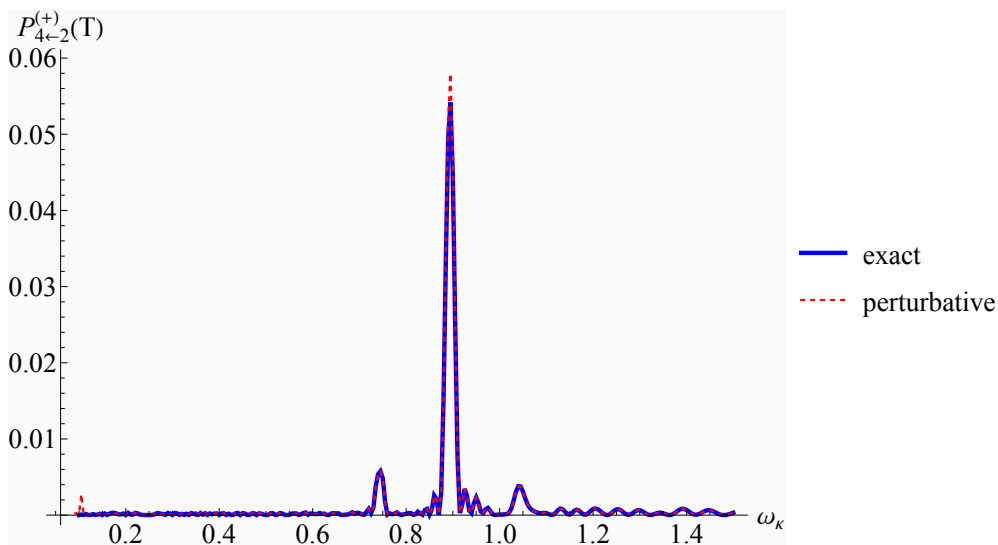


**Figure 2.** Boundary driven transition probability  $P_{4\leftarrow 2}^{(+)}(T)$  in the perturbative approximation (4.16) and exact analytical form (4.38) as a function of the modulation frequency  $\omega_\kappa$ . The parameters are  $A_f(t) = 0$ ,  $A_b(t) = 1 + 0.08 \cos(\omega_b t)$ ,  $\kappa(t) = \kappa_0 \sin(\omega_\kappa t)$ ,  $\delta(t) = \delta_0$ ,  $|g(t)| = \lambda e^{\delta(t)}/\sqrt{2\Omega}$ ,  $\omega_b = 0.3$ ,  $\kappa_0 = 0.1$ ,  $\delta_0 = 0.2$ ,  $\lambda = 0.25$ ,  $T = 2\pi 20/\omega_\kappa$ , and  $\Omega = 20$ . The dominant peak occurs near  $\omega_\kappa \simeq 0.89$ , while the smaller sideband peaks occur near  $\omega_\kappa \simeq 0.74$  and  $\omega_\kappa \simeq 1.04$ .

The dominant peak occurs when the boundary modulation satisfies the parametric resonance condition

$$2\omega_\kappa \simeq 2\overline{W}_+, \quad \overline{W}_+ = \frac{1}{T} \int_0^T W_+(t) dt, \quad (5.6)$$

or equivalently  $\omega_\kappa \simeq \overline{W}_+$ . This reflects the fact that the transition  $2 \rightarrow 4$  has energy gap  $2\overline{W}_+$ , while the boundary drive enters through the second harmonic  $2\omega_\kappa$ . The smaller peaks arise as sideband resonances, generated by the additional modulation of the RPA frequency through  $A_b(t) = 1 + 0.08 \cos(\omega_b t)$ . They are expected near

$$2\omega_\kappa \simeq 2\overline{W}_+ \pm \omega_b, \tag{5.7}$$

or equivalently  $\omega_\kappa \simeq \overline{W}_+ \pm \omega_b/2$ . For the parameters of figure 2, this gives sideband peaks near  $\omega_\kappa \simeq 0.74$  and  $\omega_\kappa \simeq 1.04$ , in agreement with the numerical plot. The figure therefore shows that the transition can also be driven directly by the moving-boundary part of the Dyson map. By tuning  $\omega_\kappa$ , the integrated transition amplitude can be enhanced or suppressed through constructive or destructive phase interference.

The comparison between the exact and the perturbative solution is similar as in the previous subsection.

## 6 Conclusion

We have studied a time-dependent non-Hermitian generalisation of the Schütte-Da Providência model and analysed its collective dynamics after a Dyson transformation and an RPA reduction. The time-dependent Dyson map maps the original non-Hermitian Hamiltonian to a Hermitian counterpart, but it does more than provide an equivalent representation. Through its explicit time dependence it generates effective driving terms in the Hermitian frame. After the RPA reduction these terms appear as time-dependent oscillator frequencies for the collective modes.

The resulting RPA eigenvalue problem yields two instantaneous oscillator branches. Their stability is determined by the reality and positivity of the corresponding frequencies  $W_\pm(t)$ . Within the stable regions the collective problem can therefore be reduced to time-dependent harmonic oscillators. This identification makes it possible to compute transition probabilities between instantaneous RPA oscillator states. In the perturbative instantaneous-basis approach, the leading transition amplitude is proportional to  $\dot{W}_j(t)/W_j(t)$ . Thus the transition  $n \rightarrow n + 2$  is purely nonadiabatic and disappears in the time-independent case, where the RPA basis is stationary.

We also derived exact transition amplitudes within the RPA approximation by using Lewis-Riesenfeld invariants. This provides a non-perturbative benchmark for the first-order instantaneous-basis result. In the weak-driving regime the two descriptions agree well and predict the same resonance positions. Near strong resonances, however, the perturbative expression overestimates the transition probability because it neglects depletion of the initial state and higher-order squeezing-induced redistribution among oscillator levels.

The numerical examples illustrate two distinct mechanisms by which the time-dependent Dyson map can drive collective transitions. A modulation of the scaling parameter  $\delta(t)$  changes the effective coupling  $g(t)$  and hence modulates the RPA frequency directly. By contrast, a modulation of the squeezing parameter  $\kappa(t)$  acts as a moving-boundary contribution and drives the system through the term proportional to  $\dot{\kappa}^2(t)$ . In both cases the

dominant transition peaks are well described as parametric resonances, while the additional smaller peaks arise from sideband mixing with the modulation of the bosonic frequency.

The main conclusion is therefore that a time-dependent Dyson map can act as a controlled driving mechanism for collective RPA modes. Even when the transformed Hamiltonian is Hermitian and the evolution is unitary in the Dyson-related frame, the explicit time dependence of the map leaves observable dynamical signatures in the form of induced collective transitions.

## References

- [1] A. Fring and M. Reboiro, Induced transitions in non-Hermitian spin-boson models with time-dependent boundaries, preprint arXiv:2605.20019 (2026).
- [2] C. M. Bender and S. Boettcher, Real Spectra in Non-Hermitian Hamiltonians Having PT Symmetry, *Phys. Rev. Lett.* **80**, 5243–5246 (1998).
- [3] C. M. Bender, Making sense of non-Hermitian Hamiltonians, *Rept. Prog. Phys.* **70**, 947–1018 (2007).
- [4] A. Mostafazadeh, Pseudo-Hermiticity versus PT symmetry: The necessary condition for the reality of the spectrum of a non-Hermitian Hamiltonian, *J. Maths. Phys.* **43**, 202–212 (2002).
- [5] A. Mostafazadeh, Pseudo-Hermitian Representation of Quantum Mechanics, *Int. J. Geom. Meth. Mod. Phys.* **7**, 1191–1306 (2010).
- [6] D. Schütte and J. Da Providencia, A solvable model of boson condensation, *Nucl. Phys. A* **282**(3), 518–532 (1977).
- [7] A. Fring and M. H. Y. Moussa, Unitary quantum evolution for time-dependent quasi-Hermitian systems with nonobservable Hamiltonians, *Phys. Rev. A* **93**(4), 042114 (2016).
- [8] A. Fring, An introduction to PT-symmetric quantum mechanics-time-dependent systems, *J. of Phys.: Conf. Series* **2448**(1), 012002 (2023).
- [9] M. Reboiro and D. Tielas, Quantum work from a pseudo-Hermitian Hamiltonian, *Quant. Rep.* **4**(4), 589–603 (2022).
- [10] D. Bohm and D. Pines, A collective description of electron interactions. I. Magnetic interactions, *Phys. Rev.* **82**(5), 625 (1951).
- [11] D. Pines and D. Bohm, A collective description of electron interactions: II. Collective vs individual particle aspects of the interactions, *Phys. Rev.* **85**(2), 338 (1952).
- [12] D. Bohm and D. Pines, A collective description of electron interactions: III. Coulomb interactions in a degenerate electron gas, *Phys. Rev.* **92**(3), 609 (1953).
- [13] K. Neergård, Nambu–Goldstone modes in the random phase approximation, *Prog. Theor. Exp. Phys.* **2016**(10), 103A01 (10 2016).

- [14] T. C. Berkelbach, Communication: Random-phase approximation excitation energies from approximate equation-of-motion coupled-cluster doubles, *J. Chem. Phys.* **149**(4), 041103 (07 2018).
- [15] M. Hellgren and L. Baguet, Random phase approximation with exchange for an accurate description of crystalline polymorphism, *Phys. Rev. Res.* **3**, 033263 (Sep 2021).
- [16] R. Folprecht, F. Knapp, G. De Gregorio, R. Mancino, P. Veselý, and N. Lo Iudice, Bulk and spectroscopic nuclear properties within an ab initio renormalized random-phase approximation framework, *Phys. Rev. C* **113**, L041302 (Apr 2026).
- [17] G. Co', Introducing the random phase approximation theory, *Universe* **9**(3), 141 (2023).
- [18] T. Holstein and H. Primakoff, Field dependence of the intrinsic domain magnetization of a ferromagnet, *Phys. Rev.* **58**, 1098–1113 (1940).
- [19] D. Rowe, Equations-of-motion method and the extended shell model, *Rev. Mod. Phys.* **40**(1), 153 (1968).
- [20] D. J. Rowe, *Nuclear collective motion: models and theory*, World Scientific, 2010.
- [21] G. D. Mahan, *Many-particle physics*, Springer, New York, 3 edition, 2008.
- [22] J.-P. Blaizot and G. Ripka, *Quantum theory of finite systems*, MIT Press, Cambridge MA, 1986.
- [23] H. Lewis and W. Riesenfeld, An Exact quantum theory of the time dependent harmonic oscillator and of a charged particle time dependent electromagnetic field, *J. Math. Phys.* **10**, 1458–1473 (1969).
- [24] I. A. Pedrosa, Canonical transformations and exact invariants for dissipative systems, *J. Maths. Phys.* **28**, 2662–2664 (1987).
- [25] A. Fring and T. Frith, Metric versus observable operator representation, higher spin models, *Eur. Phys. J. Plus* , 133: 57 (2018).